with pbFGF, pIM45, and pladeno-1 to produce the AAV inducing bFGF gene (AAV-bFGF). After 48 hr, cells were harvested and lysed in Tris-HCl buffer (10 m*M* Tris-HCl, 150 m*M* NaCl, pH 8.0) through three cycles of freezing and thawing. One round of sucrose precipitation and two rounds of CsCl density gradient ultracentrifugation were performed to isolate AAV-bFGF from the lysates. The vector titer was determined by quantitative DNA dot-blot hybridization of the DNase I-resistant fraction.

In vitro *study: examination of the potency of AAV as a viral vector when targeted at synoviocytes*

Isolation of synoviocytes. Five Japanese white rabbits (Oriental Yeast, Tokyo, Japan), 12 weeks old, weighing an average of 2.1 kg, were used for the study. Under intravenous anesthesia with pentobarbital sodium (Somnopentyl; Schering-Plough Animal Health, Union, NJ), synovial tissues were harvested from the knee joint, washed three times in phosphate-buffered saline (PBS), and cut into small pieces. These pieces were then treated with 0.25% collagenase (type II collagenase; Worthington Biochemical, Lakewood, NJ) for 2 hr at 37°C. The treated synoviocytes were washed three times with PBS and centrifuged for 5 min at 1500 rpm, and then equally divided into four separate flat-bottomed plates (Falcon [diameter, 30 mm]; BD Biosciences Discovery Labware, Bedford, MA) at 1×10^5 cells per plate in 1.0 ml of Dulbecco's modified Eagle's medium (DMEM; Sigma, St. Louis, MO) supplemented with 10% fetal calf serum (FCS) and antibiotics (penicillin G [100 U/ml] and streptomycin [0.1 mg/ml]; GIBCO-BRL Invitrogen, Carlsbad, CA) (DMEM–FCS), at 37°C in a 5% CO_2–air atmosphere for 48 hr.

Gene transduction into synoviocytes. After 48 hr in growth medium, the synoviocyte cultures were removed and washed once with serum-free DMEM. A 500-μl volume of serum-free DMEM containing AAV-LacZ was added to the control group culture plate, and 500 μl of serum-free DMEM containing AAV-bFGF was added to the gene-transduced group culture plate. This was to enable quantification of transgene expression at the optimal number of viral particles (10^7 particles per cell) determined from pilot studies (data not shown).

Five samples from the bFGF-transduced group and five from the control group (*lacZ*-transduced group) were used for the experiment to determine the efficiency of gene transduction *in vitro*. Culture medium was not exchanged during the examination period of 2 weeks. 3, 7, and 14 days after transduction, supernatant was removed, and LacZ expression in the LacZ group was assessed by the X-Gal staining technique (Yokoo *et al.*, 2005). The efficiency of gene transduction was calculated as the average percentage of X-Gal-positive cells per total living cells, determined by viewing three randomly selected fields (magnification, ×100) with an optical microscope.

Measurement of bFGF concentration in culture medium. Five samples from the bFGF-transduced group and five from the control group (*lacZ*-transduced group) were used to determine the accumulation of bFGF in culture supernatant. The culture medium of bFGF-transduced or control chondrocytes was not exchanged at each sampling. 3, 7, and 14 days after transduction, culture supernatants were collected from all four bFGF-transduced or control group culture wells and, after centrifugation, were stored at −80°C until analysis. The bFGF concentration in culture supernatants of both groups were measured by enzyme-linked immunosorbent assay (ELISA), using a bFGF-specific ELISA kit (Quantikine; R&D Systems, Minneapolis, MN) according to the manufacturer's instructions.

In vivo *study: cartilage regeneration by intraarticular administration of AAV-bFGF*

Intraarticular administration of AAV-bFGF into articular cartilage defect. Surgery and postoperative management were carried out under certification of the Yokohama City University Animal Center (Yokohama City, Japan) and with the approval of the Animal Care Committee.

Twenty-four Japanese white rabbits were used for the *in vivo* study. They were anesthetized as required by intravenous injection of pentobarbital sodium, and both knees were sterilized for surgery. A 2.5-cm medial parapatellar incision was made and the patella was dislocated laterally. A full-thickness defect (diameter, 5 mm; depth, 3 mm) was artificially created in the patellar groove of the anterior surface of the distal femur, using a hand drill bit; 1×10^9 particles (100 μl of solution containing 1×10^{10} particles/ml) of AAV-bFGF, which had been shown to be the optimal amount in our pilot study, was administered with a microsyringe, and the dislocated patella was reduced to its original position immediately. The same procedure was repeated for the contralateral knee. In the control group, the same procedure was followed, but 100 μl of phosphate-buffered saline (PBS) solution was administered instead of AAV-bFGF. The rabbits were allowed freedom of movement immediately after surgery. Four rabbits from each group were subsequently killed at 4, 8, and 12 weeks for macroscopic and histological examination of the articular surface of both knees.

Macroscopic and histological evaluation of repaired cartilage. To enable comparative examination of the articular components, four animals (both knees) from the AAV-bFGF group, and an equivalent number from the PBS (control) group, were sacrificed at 4, 8, and 12 weeks. Macroscopic assessment and photography were followed by *en bloc* resection of the distal end of the femur. The specimens were fixed with 10% buffered formaldehyde for 1 week, followed by decalcification with 0.5 *M* EDTA solution for 2 to 3 weeks. Sagittal sections through cartilaginous tissue and bone were prepared and stained with hematoxylin and eosin (H&E) and safranin O. Macroscopic findings for each specimen were evaluated semiquantitively according to the scale described by Kumagai *et al.* (2003). The Kumagai Scale for Macroscopic Assessment of Cartilage Surface is an established system of parameters for grading specimens in color (0–3), connection of new tissue to adjacent cartilage (0–2), size of remaining defect (0–5), depression of the defect (0–4), and depth of the defect (0–2). The overall score scales from zero, suggesting full repair, to 16, indicating no repair.

Likewise, histological findings for each specimen were evaluated semiquantitatively according to the scale described by Wakitani *et al.* (1994). The Wakitani Scale for Histological As-

sessment of Cartilage Defects is an established system of parameters for grading specimens in cell morphology (0–4), matrix staining (0–3), surface regularity (0–3), thickness of cartilage (0–2), and integration of donor with adjacent host cartilage (0–2). The overall score scales from zero, suggesting full repair, to 14, indicating no repair.

Evaluation of supernatant bFGF concentration after in vivo *study.* At the time of sacrifice, synovial tissue was harvested for examination of bFGF concentration after *in vivo* administration of AAV-bFGF. Harvested tissues were treated with 0.25% type II collagenase as previously described, and cultured for 1 week at 37°C without exchange of medium. Supernatant of the synoviocyte cultures from the bFGF group and from the control group were analyzed at 4, 8, and 12 weeks and evaluated by the ELISA method.

Immunohistological assessment for type II collagen in cell matrix. Immunohistological assessment targeted the type II collagen seen in the extracellular matrix of the regenerated cartilage, using rabbit anti-type II collagen antibody (Santa Cruz Biotechnology, Santa Cruz, CA).

Statistical analysis. Data were expressed as means ± standard deviation (SD). The statistical significance of differences was calculated with StatView version J-5.0 (SAS Institute, Cary, NC). One-way analysis of variance (ANOVA) and the Mann–Whitney U test were used for analyzing statistical significance. p Values less than 0.05 were considered significant.

RESULTS

In vitro *study: examination of the potency of AAV as a viral vector when targeted at synoviocytes*

Efficiency of gene transduction into synoviocytes: LacZ expression. Values for synoviocytes transfected with AAV-LacZ were determined at intervals of 3, 7, and 14 days after transduction. The percentage of LacZ-positive cells among total living cells was determined to be 55.8 ± 6.0 (mean ± SD), 83.4 ± 3.8, and 92.0 ± 1.6%, respectively, at an optimal dose of 10^7 particles per cell (Table 1). The percentage of successfully transduced synoviocytes increased in a vector dose-dependent manner up to an optimal figure of 10^7 particles per cell, when approximately 100% efficiency was achieved. Doses of viral particles above that level failed to improve the transduction rate. Microscopic examination did not reveal any evidence of cell death or cytopathic change in the transduced cells.

bFGF gene expression in transduced synoviocytes. bFGF production was detected in both bFGF-transduced and control cells. bFGF concentration in the culture supernatant was 31.2 ± 7.8, 80.5 ± 16.4, and 120.8 ± 22.5 ng/ml at 3, 7, and 14 days after transduction, respectively, in bFGF-transduced cells (Table 1). In control cells, the bFGF concentration was 22.6 ± 9.2, 23.1 ± 6.4, and 28.4 ± 7.8 ng/ml at 3, 7, and 14 days after transduction, respectively. The bFGF concentration was significantly greater in bFGF-transduced cells than in control cells at each sampling time point ($p < 0.01$).

In vivo *study: cartilage regeneration by intraarticular administration of AAV-bFGF*

Macroscopic findings on cartilage regeneration. Observation of the articular cartilage defect site showed regeneration in both the bFGF-transduced and control groups. At 4 weeks, cartilage regeneration was not obvious in the control group (Fig. 1A), whereas partial coverage by regenerated cartilage was seen in the AAV-bFGF group (Fig. 1B). At 8 weeks, the difference in cartilage regeneration became more apparent (Fig. 1C and D) and at 12 weeks, the margin between the regenerated tissue and the original cartilage was not distinguishable in the AAV-bFGF group (Fig. 1F), whereas the margin was clearly visible in the control group (Fig. 1E).

Histological findings on cartilage regeneration. At 4 weeks after administration of AAV-bFGF, tissues obtained from the bFGF-transduced group showed slight formation of a chondral layer in the deep part of the cartilage defect. Tissue was composed of round chondrocytes with weakly safranin O-stained extracellular matrix (Fig. 2B). There was no integration of the edges of regenerated tissue with normal adjacent cartilage or reconstitution of the osteochondral junction in any specimen. In the control group, the extracellular matrix was hardly stained with safranin O (Fig. 2A), and no cartilage regeneration was

TABLE 1. TIME-DEPENDENT LacZ EXPRESSION AND SUPERNATANT bFGF CONCENTRATION IN CULTURED SYNOVIOCYTES[a]

Days after transfection	*Percentage of LacZ-positive cells*	*bFGF concentration (ng/ml)*	
		AAV-bFGF group[b]	*Control group*[b]
3	55.8 ± 6.0	31.2 ± 7.8	22.6 ± 9.2
7	83.4 ± 3.8	80.5 ± 16.4	23.1 ± 6.4
14	92.0 ± 1.6	120.8 ± 22.5	28.4 ± 7.8

[a]LacZ expression was assessed by X-Gal staining 3, 7, and 14 days after AAV-LacZ transduction of chondrocytes. Values represent mean percentages ± SD. bFGF concentration of the supernatant was analyzed by ELISA 3, 7, and 14 days after AAV-bFGF transduction of synoviocytes. Values represent mean concentrations (ng/ml) ± SD. $n = 5$.

[b]$p < 0.01$.

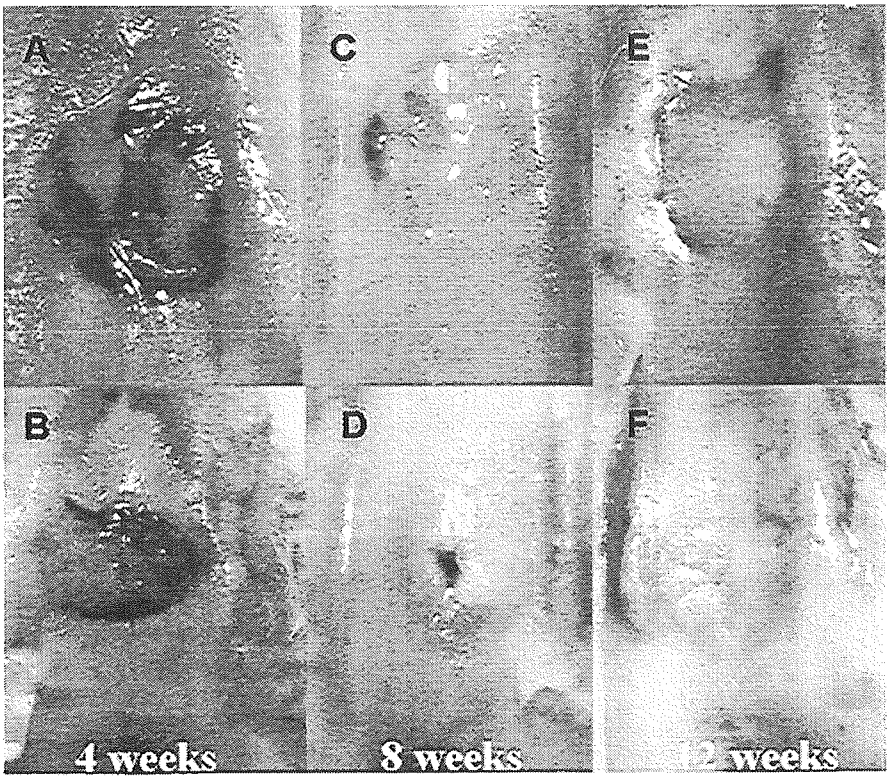

FIG. 1. Macroscopic photographs showing cartilage repair after interarticular administration of AAV-bFGF and control at 4, 8, and 12 weeks after operation. At 12 weeks in the AAV-bFGF group, almost complete repair is seen, whereas in the control group, the margin between the newly formed cartilage and the surrounding normal cartilage is obvious.

seen. The tissues showed inflammatory granulation of the defect area, and any bone may have been partly obscured because of apoptosis and replacement of fibrous tissues.

At 8 weeks, in the bFGF-transduced group, the extracellular matrix was more distinctly stained with safranin O, and cartilage regeneration was seen not only in the deep part, but also in the superficial layer (Fig. 2D). Both edges of the regenerated cartilage showed almost complete integration with normal adjacent cartilage, and reconstitution of the osteochondral junction was seen in five specimens. In Fig. 2C, tissues from the control group were essentially the same as those seen at 4 weeks. Although safranin O staining appears stronger, there is no apparent formation of hyaline cartilage and no construct of mature cartilage tissue is visible.

In the bFGF-transduced group at 12 weeks, the intensity and thickness of the extracellular matrix were increased when compared with the findings at 4 and 8 weeks, and the microstructure of the regenerated tissue resembled the surrounding normal cartilage (Fig. 2F). There was reconstitution of the osteochondral junction in most specimens, and formation of the surface layer of articular cartilage was distinctly more pronounced in contrast to that shown in the control (Fig. 2E). In the control group, formation of hyaline cartilage-like tissue was seen in three specimens, but others presented formation of fibrous cartilage. Extracellular matrix stained well with safranin O in three specimens, but was less compared with the bFGF group. There was no reconstitution of the osteochondral junction in any specimen.

Semiquantitive macroscopic and histological analyses. Semiquantitive analysis using the Kumagai Scale showed a significant difference in the two groups ($p < 0.01$) as detailed in Table 2. At 4, 8, and 12 weeks, average macroscopic scores in the AAV-bFGF group were 9.25 ± 2.21, 2.25 ± 0.70, and 0.25 ± 0.12 points, and the surface of the regenerated cartilage closely resembled normal cartilage in the bFGF-transduced group. On the other hand, macroscopic scores in the control group showed an average of 12.0 ± 2.34, 8.50 ± 1.72, and 5.00 ± 1.28 points at 4, 8, and 12 weeks, respectively, and regenerated cartilage could still be distinguished from surrounding normal cartilage even at 12 weeks. No sign of osteoarthrosis, such as erosion of cartilage or formation of osteophytes, was recognized in any of the joint surfaces during the observation period. Tumor formation was also not recognized, but there was a slight hyperplastic change in the lateral condyle in one knee joint of the bFGF group. No hyperplasia of synovium was seen in any of the joints of the bFGF-transduced group.

Histological analysis using the Wakitani score showed 6.75 ± 1.15, 2.25 ± 0.67, and 0.75 ± 0.33 points at 4, 8, and 12 weeks after AAV-bFGF administration, respectively (Table 2). In the control group, the score was 13.5 ± 1.0, 11.0 ± 1.5, and 5.00 ± 2.00 points at 4, 8, and 12 weeks respectively. The scores in both groups decreased throughout the experimental period. However, the score in the bFGF-transduced group became significantly lower than that in the control group over time ($p < 0.01$).

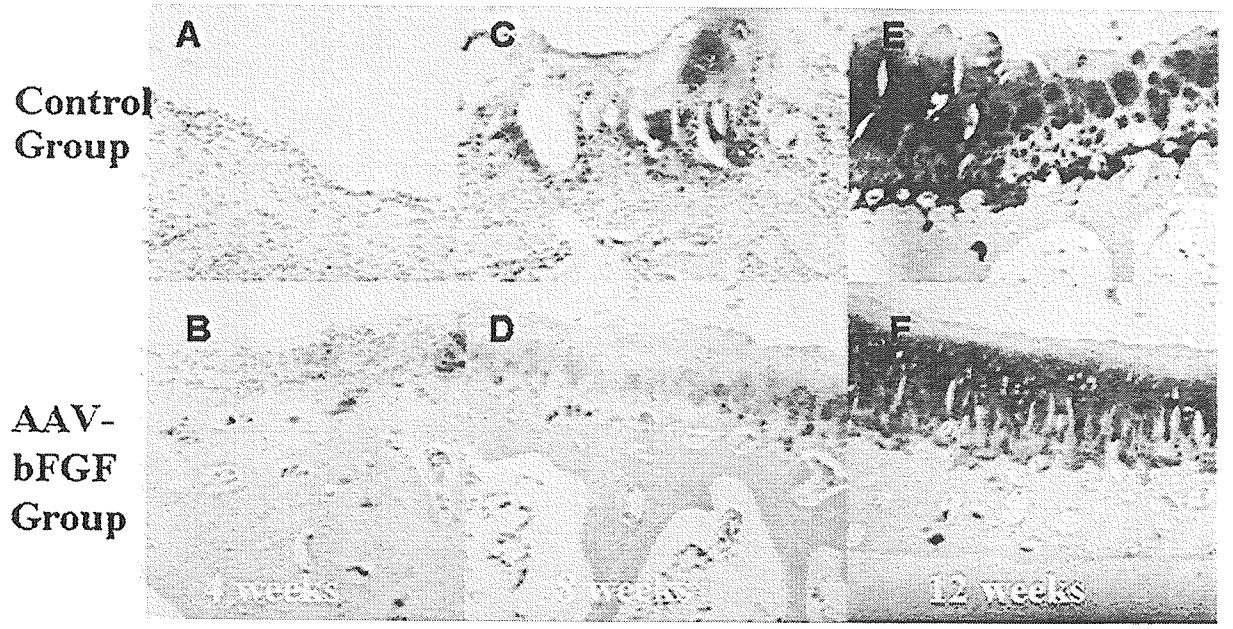

FIG. 2. Histological assessment of prepared sagittal sections using safranin O and hematoxylin staining. At 4 weeks (**A**) control group extracellular matrix is hardly stained, no cartilage regeneration is seen, but the tissues show inflammatory granulation of the defect area, which may obscure any bone because of apoptosis and replacement of fibrous tissue. (**B**) bFGF-transduced group matrix is lightly stained and the deep part is composed of rounded chondrocytes. At 8 weeks (**C**) partial chondrocyte repair is seen, with limited metachromasy. (**D**) The matrix is more distinctly stained and cartilage regeneration has advanced to the superficial layer. At 12 weeks (**E**) generation of chondrocyte-like cells with irregular matrix formation is seen, but no reconstitution of the bone–cartilage junction is apparent. (**F**) Note the intensely stained matrix, reconstitution of the osteochondral junction, and formation of the surface layer of the articular cartilage.

bFGF concentration in synovial cell culture after in vivo *administration of AAV-bFGF.* bFGF production was detected in both bFGF-transduced and control cells. bFGF concentration in the culture supernatant was 133.8 ± 15.6, 122.5 ± 19.3, and 94.0 ± 8.4 ng/ml at 4, 8, and 12 weeks after transduction, respectively, in bFGF-transduced cells (Fig. 3). In control cells, bFGF concentration was 34.0 ± 7.8, 19.5 ± 6.3, and 21.0 ± 2.7 ng/ml at 4, 8, and 12 weeks after transduction, respectively. bFGF concentration was significantly greater in bFGF -transduced cells than in control cells on all days of sampling ($p < 0.01$).

Immunohistological assessment of the cell matrix. Immunohistological assessment of the extracellular matrix was made in the AAV-bFGF group at 8 and 12 weeks. The antibody was targeted at extracellular matrix, and clear staining was seen at both 8 and 12 weeks, when compared with the control group (Fig. 4).

DISCUSSION

Because of its limited self-repairing nature, regeneration of cartilage is a difficult task, and clinical attempts have been made

TABLE 2. SEMIQUANTITIVE MACROSCOPIC AND HISTOLOGICAL ANALYSIS OF bFGF-TRANSDUCED CARTILAGE[a]

Weeks after transduction	*Macroscopic score*[b]		*Histological score*[b]	
	AAV-bFGF-F	*Control*	*AAV-bFGF*	*Control*
4	9.25 ± 2.21	12.0 ± 2.34	6.75 ± 1.15	13.5 ± 1.00
8	2.25 ± 0.70	8.50 ± 1.72	2.25 ± 0.67	11.0 ± 1.50
12	0.25 ± 0.12	5.00 ± 1.28	0.75 ± 0.33	5.00 ± 2.00

[a]Semiquantitive macroscopic and histological scores comparing the AAV-bFGF group and control group at 4, 8, and 12 weeks after administration. Macroscopic scoring system: 0 points, maximum with complete repair; 16 points, minimum with no repair. Histological scoring system: maximum and minimum scores are 0 and 14 points, respectively. $n = 8$.

[b]$p < 0.01$.

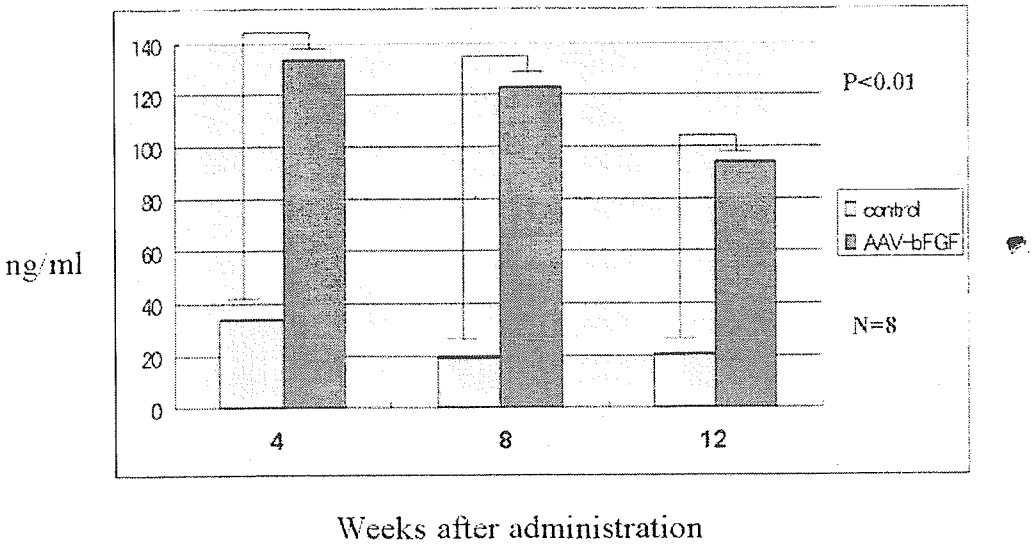

FIG. 3. bFGF concentration in culture supernatant of bFGF-transduced synoviocytes 4, 8, and 12 weeks after AAV-bFGF administration. Culture supernatants of control and bFGF-transduced cells were collected 7 days after harvesting and culture, and bFGF concentration was determined by ELISA. Transduction of the bFGF gene significantly elevates the secretion of bFGF ($*p < 0.01$).

to repair human cartilage, such as implantation of autologous chondrocytes (Richardson *et al.*, 1999), which have proven successful. In these cases, autologous chondrocyte grafts, harvested from non-weight-bearing areas, were cultured *in vitro* and then reinserted into the cartilage defect with coverage by a periosteal flap. However, because of the limited amount of graft tissue that can be obtained from the donor site, the method is limited to small local cartilage defects. Another successful method used clinically is mosaicplasty, used in diseases such as osteochondritis dissecans, but again, patients are limited to those who suffer only from small local cartilage defects. Given these limitations, a more fundamental method for cartilage repair would seem to be needed.

With numerous studies concerning growth factors, and discovery of potent gene transporters, methods to transport these genes into target organs have come to light (Kaplitt *et al.*, 1994; Berns and Giraud, 1995; Xiao *et al.*, 1997; Schwarz, 2000). Thus, gene therapy has become one of the most powerful tools for treatment of degenerative disorders, but still has several problems: the first, and perhaps most important, is that of safety—that is, in terms of virus virulence and their ability to self-reproduce; the second concerns their capacity to integrate into the host genome; and the third is the issue of long-term gene expression.

Adeno-associated virus (AAV), which was first discovered in research of its hosting virus, the adenovirus, has several bi-

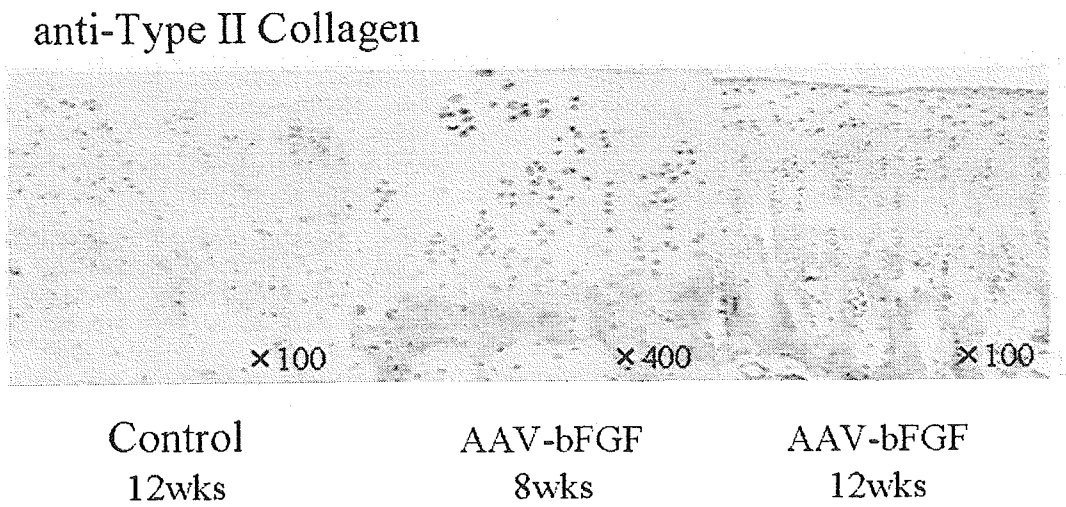

FIG. 4. Immunohistological staining for type II collagen. Staining is not seen in the negative control at 12 weeks. Staining of the extracellular matrix is seen at 8 weeks, and is most strong 12 weeks after AAV-bFGF administration.

ological advantages over other viral gene transporters, and the only apparent disadvantage is its small size, which may limit the size of the gene it can carry. It is most important to obtain high-efficiency transduction and continuous local expression of the therapeutic gene for repair of cartilage defects by gene therapy. Several studies have demonstrated the high ability of the AAV as a gene transporter, and its ability to express the transduced gene for a certain length of time (Kessler *et al.*, 1996; Fisher *et al.*, 1997; Herzog *et al.*, 1997). There are also reports of the utility of the AAV vector in the treatment of joint diseases, in which it demonstrated high-efficiency gene delivery into the synovium *in vivo* (Goater *et al.*, 2000), and gene transduction into cultured chondrocytes *in vitro* (Arai *et al.*, 2000). In our previous study, *ex vivo* gene transfer to periosteum-derived cells, using an AAV vector, induced *lacZ* gene expression for 4 weeks *in vivo* (Kobayashi *et al.*, 2002). However, the *ex vivo* method is complex, and may not be practical in terms of clinical therapy. On the other hand, delivering genes directly to the surface of abnormal articular cartilage could result in long-term treatment to accelerate cartilage repair.

Augmentation of cartilage repair by application of basic fibroblast growth factor (bFGF) has been reported to be efficient (Shida *et al.*, 1996; Cuevas *et al.*, 1988). Weisser *et al.* (2001) documented that by transplanting chondrocytes treated with several growth factors, positive effects on cartilage repair were observed only in bFGF-treated chondrocyte implants, and Fujimoto *et al.* (1999) showed that *in situ* delivery of bFGF also enhanced the ability to repair cartilage. Other studies have also shown that exogenous bFGF induced proliferation of chondrocytes, maturation of cartilage, and differentiation of mesenchymal cells, and stimulated synthesis of cartilaginous matrix (Cuevas *et al.*, 1988; Shida *et al.*, 1996). Otsuka *et al.* (1997) described how continuous administration of bFGF, using an osmotic pump, had a clear beneficial effect on repair of cartilage defects.

After considering the above-described findings, we were led to believe that achieving integration of the bFGF gene into intraarticular tissues, such as synoviocytes, by intraarticular administration could result in long-term expression and prolonged secretion of the growth factor, and culminate in regeneration of cartilage.

In this study, high-efficiency *lacZ* gene transduction to synoviocytes was obtained *in vitro*, and bFGF gene expression was detected in both bFGF-transduced and control cells. Subsequently, gene expression *in vivo* was sustained for at least 12 weeks without any adverse effects, and the findings suggest that *in vivo* gene transfer to articular cartilage defects, using the AAV vector, was successful.

We have shown that bFGF secretion was significantly increased in bFGF-transduced synoviocytes compared with the control groups, both *in vitro* and *in vivo*. Furthermore, repair at a relatively early stage was noticeably different between the bFGF-transduced and control cartilage tissue, and the eventual histological appearance of the transfected site in the bFGF-transduced group showed full repair compared with the control group, where the difference was still visible.

The results demonstrate that repair of full-thickness defects in rabbit articular cartilage can be enhanced by intraarticular administration of AAV-bFGF, by a procedure that is much less complex compared with the orthodox *ex vivo* method, and that is equally, if not more, effective.

Hence, it can be concluded that continuous bFGF secretion by gene transfer was extremely effective in promoting cartilage repair, demonstrating that this approach could in future be used clinically as a potent method for repair of cartilaginous diseases. However, further long-term studies will be necessary to assess the final outcome of regenerated articular cartilage.

ACKNOWLEDGMENTS

Supported in part by grants from the Grant-in-Aid for Scientific Research from the Ministry of Education, Culture, Sports, Science, and Technology of Japan.

REFERENCES

ARAI, Y., KUBO, T., KOBAYASHI, K., TAKESHITA, K., TAKAHASHI, K., IKEDA, T., IMANISHI, J., TAKIGAWA, M., and HIRASAWA, Y. (1997). Adenovirus vector-mediated gene transduction to chondrocytes: *In vitro* evaluation of therapeutic efficiency of transforming growth factor-β_1 and heat shock protein 70 gene transduction. J. Rheumatol. **24,** 1787–1795.

ARAI, Y., KUBO, T., FUSHIKI, S., MAZDA, O., NAKAI, H., IWAKI, Y., IMANISHI, J., and HIRASAWA, Y. (2000). Gene delivery to human chondrocytes by an adeno-associated virus vector. J. Rheumatol. **27,** 979–982.

BARAGI, V.M., RENKIEWICZ, R.R., QIU, L., BRAMMER, D., RILEY, J.M., SIGLER, R.E., FRENKEL, S.R., AMIN, A., ABRAMSON, S.B., and ROESSLER, B.J. (1997). Transplantation of adenovirally transduced allogenic chondrocytes into articular cartilage defects *in vivo*. Osteoarthritis Cartilage **5,** 275–282.

BERNS, K.I., and GIRAUD, C. (1995). Adenovirus and adeno-associated virus as vectors for gene therapy. Ann. N.Y. Acad. Sci. **772,** 95–104.

BRITTBERG, M., LINDAHL, A., NILSSON, A., OHLSSON, C., ISAKSSON, O., and PETERSON, L. (1994). Treatment of deep cartilage defects in the knee with autologous chondrocyte transplantation. N. Engl. J. Med. **331,** 889–895.

CUEVAS, P., BURGOS, J., and BAIRD, A. (1988). Basic fibroblast growth factor (FGF) promotes cartilage repair *in vivo*. Biochem. Biophys. Res. Commun. **156,** 611–618.

DOHERTY, P.J., ZHANG, H., TREMBLAY, L., MANOLOPOULOS, V., and MARSHALL, K.W. (1998). Resurfacing of articular cartilage explants with genetically modified human chondrocytes *in vitro*. Osteoarthritis Cartilage **6,** 153–159.

FISHER, K.J., JOOSS, K., ALSTON, J., YANG, Y., HAECKER, S.E., HIGH, K., PATHAK, R., RAPER, S.E., and WILSON, J.M. (1997). Recombinant adeno-associated virus for muscle directed gene therapy. Nat. Med. **3,** 306–312.

FUJIMOTO, E., OCHI, M., KATO, Y., MOCHIZUKI, Y., SUMEN, Y., and IKUTA, Y. (1999). Beneficial effect of basic fibroblast growth factor on the repair of full-thickness defects in rabbit articular cartilage. Arch. Orthop. Trauma Surg. **119,** 139–145.

GOATER, J., MULLER, R., KOLLIAS, G., FIRESTEIN, G.S., SANZ, I., O'KEEFE, R.J., and SCHWARZ, E.M. (2000). Empirical advantages of adeno associated viral vectors for *in vivo* gene therapy for arthritis. J. Rheumatol. **27,** 983–989.

HERZOG, R.W., HAGSTROM, J.N., KUNG, S.H., TAI, S.J., WILSON, J.M., FISHER, K.J., and HIGH, K.A. (1997). Stable gene transfer and expression of human blood coagulation factor IX after intramuscular injection of recombinant adeno-associated virus. Proc. Natl. Acad. Sci. U.S.A. **94,** 5804–5809.

HUNZIKER, E.B., and ROSENGERG, L.C. (1996). Repair of partial-thickness defects in articular cartilage: Cell recruitment from the synovial membrane. J. Bone Joint Surg. Am. **78,** 721–733.

KANG, R., MARUI, T., GHIVIZZANI, S.C., NITA, I.M., GEORGESCU, H.I., SUH, J.K., ROBBINS, P.D., and EVANS, C.H. (1997). *Ex vivo* gene transfer to chondrocytes in full-thickness articular cartilage defects: A feasibility study. Osteoarthritis Cartilage **5,** 139–143.

KAPLITT, M.G., LEONE, P., SAMULSKI, R.J., XIAO, X., PFAFF, D.W., O'MALLEY, K.L., and DURING, M.J. (1994). Long-term gene expression and phenotypic correction using adeno-associated virus vectors in the mammalian brain. Nat. Genet. **8,** 148–154.

KESSLER, P.D., PODSAKOFF, G.M., CHEN, X., MCQUISTON, S.A., COLOSI, P.C., MATELIS, L.A., KURTZMAN, G.J., and BYRNE, B.J. (1996). Gene delivery to skeletal muscle results in sustained expression and systemic delivery of a therapeutic protain. Proc. Natl. Acad. Sci. U.S.A. **93,** 14082–14087.

KOBAYASHI, N., KOSHINO, T., UESUGI, M., YOKOO, N., XIN, K.Q., OKUDA, K., MIZUKAMI, H., OZAWA, K., and SAITO, T. (2002). Gene marking in adeno-associated virus vector infected periosteum-derived cells for cartilage repair. J. Rheumatol. **29,** 2176–2180.

KUMAGAI, K., SAITO, T., and KOSHINO, T. (2003). Articular cartilage repair of rabbit chondral defect promoted by creation of periarticular bony defect. J. Orthop. Sci. **8,** 700–706.

OTSUKA, Y., MIZUTA, H., TAKAGI, K., IYAMA, K., YOSHITAKE, Y., NISHIKAWA, K., SUZUKI, F., and HIRAKI, Y. (1997). Requirement of fibroblast growth factor signaling for regeneration of epiphyseal morphology in rabbit full-thickness defects of articular cartilage. Dev. Growth Differ. **39,** 143–156.

PRICE, J., TURNER, D., and CEPKO, C. (1987). Lineage analysis in the vertebrate nervous system by retrovirus-mediated gene transfer. Proc. Natl. Acad. Sci. U.S.A. **84,** 156–160.

RICHARDSON, J.B., CATERSON, B., EVANS, E.H., ASHTON, B.A., and ROBERTS, S. (1999). Repair of human articular cartilage after implantation of autologous chondrocytes. J. Bone Joint Surg. Br. **81,** 1064–1068.

SCHWARZ, E.M. (2000). The adeno-associated virus vector for orthopaedic gene therapy. Clin. Orthop. **379S,** 31–39.

SHIDA, J., JINGUSHI, S., IZUMI, T., IWAKI, A., and SUGIOKA, Y. (1996). Basic fibroblast growth factor stimulates articular cartilage enlargement in young rats *in vivo*. J. Orthop. Res. **14,** 265–272.

WAKITANI, S., GOTO, T., PINEDA, S.J., YOUNG, R.G., MANSOUR, J.M., CAPLAN, A.I., and GOLDBERG, V.M. (1994). Mesenchymal cell-based repair of large, full-thickness defects of articular cartilage. J. Bone Joint Surg. Am. **76,** 579–592.

WEISSER, J., RAHFOTH, B., TIMMERMANN, A., AIGNER, T., BRAUER, R., and VON DER MARK, K. (2001). Role of growth factors in rabbit articular cartilage repair by chondrocytes in agarose. Osteoarthritis Cartilage **9**(Suppl. A), S48–S54.

XIAO, X., LI, J., MCCOWN, T.J., and SAMULSKI, R.J. (1997). Gene transfer by adeno-associated virus vectors into the central nervous system. Exp. Neurol. **144,** 113–124.

YOKOO, N., SAITO, T., UESUGI, M., KOBAYASHI, N., XIN, K.Q., OKUDA, K., MIZUKAMI, H., OZAWA, K., and KOSHINO, T. (2005). Repair of articular cartilage defect by autologous transplantation of basic fibroblast growth factor gene-transduced chondrocytes with adeno-associated virus vector. Arthritis Rheum. **52,** 164–170.

Address reprint requests to:
Dr. Atsuo Hiraide
Department of Orthopedic Surgery
Yokohama City University School of Medicine
3-9 Fukuura, Kanazawa-ku
Yokohama 236-0004, Japan

E-mail: arzt2001@h9.dion.ne.jp

Received for publication August 3, 2005; accepted after revision October 12, 2005.

Published online: November 4, 2005.

HUMAN GENE THERAPY 16:1212–1218 (October 2005)
© Mary Ann Liebert, Inc.

Technical Report

Large-Scale Production of Recombinant Viruses by Use of a Large Culture Vessel with Active Gassing

TAKASHI OKADA,[1] TATSUYA NOMOTO,[1] TORU YOSHIOKA,[1] MUTSUKO NONAKA-SARUKAWA,[1] TAKAYUKI ITO,[1] TSUYOSHI OGURA,[1] MAYUMI IWATA-OKADA,[2] RYOSUKE UCHIBORI,[1] KUNIKO SHIMAZAKI,[3] HIROAKI MIZUKAMI,[1] AKIHIRO KUME,[1] and KEIYA OZAWA[1,2]

ABSTRACT

Adenovirus and adeno-associated virus (AAV) vectors are increasingly used for gene transduction experiments. However, to produce a sufficient amount of these vectors for *in vivo* experiments requires large-capacity tissue culture facilities, which may not be practical in limited laboratory space. We describe here a large-scale method to produce adenovirus and AAV vectors with an active gassing system that uses large culture vessels to process labor- and cost-effective infection or transfection in a closed system. Development of this system was based on the infection or transfection of 293 cells on a large scale, using a large culture vessel with a surface area of 6320 cm^2. A minipump was connected to the gas inlet of the large vessel, which was placed inside the incubator, so that the incubator atmosphere was circulated through the vessel. When active gassing was employed, the productivity of the adenovirus and AAV vectors significantly increased. This vector production system was achieved by improved CO_2 and air exchange and maintenance of pH in the culture medium. Viral production with active gassing is particularly promising, as it can be used with existing incubators and the large culture vessel can readily be converted for use with the active gassing system.

OVERVIEW SUMMARY

Large-scale production of recombinant viruses, using a large culture vessel with active gassing, is superior to protocols using standard tissue culture plates or flasks because of the higher capacity for cell growth. Although a previous protocol for recombinant virus production in a large culture vessel had the problem of insufficient transduction efficiency resulting from inadequate gas exchange, a method to use active gassing successfully improved productivity of recombinant viruses. Development of a vector production system on a large scale, using commercially available large culture vessels, allows us to process labor- and cost-effective manipulation in a closed system.

INTRODUCTION

ADENOVIRUS AND ADENO-ASSOCIATED VIRUS (AAV) VECTORS are highly efficient for transduction in many gene therapy studies (Okada *et al.*, 2002b, 2004; Ito *et al.*, 2003; Nomoto *et al.*, 2003; Yamaguchi *et al.*, 2003; Mochizuki *et al.*, 2004; Yoshioka *et al.*, 2004; Liu *et al.*, 2005). However, current production methods rely on the manipulation of many individual flasks and are not generally considered appropriate for scaling-up of production because it would be a time-consuming and labor-intensive process. Therefore, alternative tissue culture vessels with higher capacity for cell growth, such as a 10-tray Cell Factory (CF10; Nalge Nunc International, Rochester, NY) with a surface area of 6320 cm^2, could be suitable for scaling-up of

[1]Division of Genetic Therapeutics, Center for Molecular Medicine, Jichi Medical School, Tochigi 329-0498, Japan.
[2]Division of Hematology, Department of Medicine, Jichi Medical School, Tochigi 329-0498, Japan.
[3]Department of Physiology, Jichi Medical School, Tochigi 329-0498, Japan.

vector production (Okada *et al.*, 2002a). This device is easy to handle and can be used for efficient cell culture on a large scale in a closed system requiring only an air filter (Berger *et al.*, 2002; Tuyaerts *et al.*, 2002). Nevertheless, a previous protocol for recombinant virus production in the CF10 had the problem of insufficient scaling-up of vector production (Liu *et al.*, 2003). In that protocol, inadequate gas exchange between the culture vessel and the incubator might have been the cause of the inefficient yield.

We consequently adapted an active gassing system to generate large numbers of recombinant viruses in the CF10. The purpose of this active gassing is to control and maintain CO_2 tension and pH in the growth medium by passing a gas mixture through the CF10. For many types of cells, pH is an important parameter for controlling cell growth. This can be achieved by gassing with CO_2 in atmospheric air in the incubator. Enhanced gas exchange in a large culture vessel should improve both viral infectivity and plasmid transfection efficiency. In combination with the previously described method of using the CF10 (Okada *et al.*, 2002a), we have now created a simple and highly efficient system of producing vector stock on a large scale. Presented here is a labor- and cost-effective method for large-scale production of adenovirus and AAV vectors with an active gassing system that uses a large culture vessel to achieve transfection or infection in a closed system.

MATERIALS AND METHODS

Cell culture with active gassing

Propagation of vectors was based on the infection or transfection of human embryonic kidney-derived 293B cells (Yamaguchi *et al.*, 2003) by using either a flask with a surface area of 225 cm^2 (Falcon, T-225; BD Biosciences Discovery Labware, Bedford, MA) or the CF10, as described previously (Okada *et al.*, 2002a). Cells were cultured in Dulbecco's modified Eagle's medium and nutrient mixture F12 (DMEM–F12: Invitrogen, Grand Island, NY) with 10% fetal bovine serum (FBS; Sigma-Aldrich, St. Louis, MO), penicillin (100 units/ml), and streptomycin (100 μg/ml) at 37°C in a 5% CO_2 incubator. First, cells were plated at 2.3×10^6 cells per T-225 or at 6.5×10^7 cells per CF10 to achieve a monolayer at 20 to 40% confluency when cells initially attach to the surface of the flask. The volume of medium used per flask was 40 ml per T-225 or 1120 ml per CF10. Subsequently, cells were grown to a confluency of 70–90% over the next 48 to 72 hr for adenovirus infection or plasmid transfection. An aquarium pump (NISSO, Tokyo, Japan) was used to circulate air through the CF10 with 5% CO_2 and humidity control by an incubator. The CF10 was mounted with a bacterial air filter (bacterial air vents; Pall Gelman Sciences, Ann Arbor, MI) to connect the aquarium pump. The pump was connected to the gas inlet of the CF10 and the CF10 was placed inside the incubator, so that the incubator atmosphere was circulated through the CF10. The flow through the CF10 was maintained at 500 ml/min. Culture medium was sampled periodically, and the CO_2 concentrations and pH were estimated with a blood gas analyzer (Nova PHOX; Diamond Diagnostics, Holliston, MA). Glucose levels of the culture medium were also estimated with a glucose meter (Glutest Sensor, Glutest Ace GT-1640; Sanwa Kagaku Kenkyusho, Nagoya, Japan).

Construction and propagation of adenoviral vectors

A recombinant adenoviral vector, Ad-EGFP, was constructed using an adenoviral DNA–protein complex without a transgene insert (AVC2.null) (Okada *et al.*, 1998); it carried the cytomegalovirus (CMV) promoter, cloning sites, a simian virus 40 (SV40) intron, and the SV40 polyadenylation signal. To generate Ad-EGFP encoding enhanced green fluorescent protein (EGFP), a *Spe*I–*Cla*I fragment containing the *EGFP* cDNA excised from pEGFP-1 (BD Biosciences Clontech, Palo Alto, CA) was inserted into the *Xba*I and *Nsp*V sites in the DNA–protein complex, AVC2.null, using the direct *in vitro* ligation technique (Okada *et al.*, 1998). The ligated DNA–protein complex was introduced into 293 cells by the calcium phosphate transfection method. Viral plaques on 293 cells were isolated, amplified, and titrated by standard techniques. To amplify the vector in 293 cells, half the medium in the tissue culture flasks was exchanged with fresh DMEM–F12 containing 10% FBS 1 hr before infection. Cells were infected with the virus at 10 multiplicities of infection (MOI) per cell. Cells were incubated to reach full cytopathic effect, and crude viral lysate was purified by two rounds of CsCl two-tier centrifugation. The average number of plaque-forming units (PFU) was assessed on the basis of the 50% tissue culture infective dose. The number of vector particles was estimated by dot-blot hybridization of DNase I-treated stocks with plasmid standards.

Construction and propagation of AAV vectors

AAV1-EGFP, a recombinant AAV type 1 expressing the *EGFP* gene under the control of the CAG promoter (modified chicken β-actin promoter) with the CMV-IE enhancer, was generated by the following procedure. A *Bam*HI–*Xba*I fragment containing EGFP cDNA excised from pEGFP-1 and a *Hin*dIII fragment containing the woodchuck hepatitis virus posttranscriptional regulatory element (WPRE) sequence excised from pBluescript II SK(+)WPRE-B11 (a gift from T. Hope, University of Illinois at Chicago, Chicago, IL) was cloned into an *Xho*I site of pCAGGS (a gift from J.-i. Miyazaki, Osaka University Graduate School of Medicine, Japan) to create pCAG-EGFP-WPRE, using an *Xho*I linker. The EGFP expression cassette in pCAG-EGFP-WPRE was ligated to *Not*I-excised pAAV-LacZ to form the proviral vector plasmid pAAV2-CAG-EGFP-WPRE. AAV viral stocks were prepared according to a previously described protocol (Okada *et al.*, 2002a) with minor modifications. Half the medium in tissue culture flasks was exchanged with fresh DMEM–F12 containing 10% FBS 1 hr before plasmid transfection. Subsequently, cells were cotransfected with 23 μg (per T-225) or 650 μg (per CF10) of each of the following plasmids: a proviral vector plasmid, AAV-1 chimeric helper plasmid p1RepCap (Mochizuki *et al.*, 2004), and adenoviral helper plasmid pAdeno, by a calcium phosphate coprecipitation method. Each of the vector and helper plasmids was added to 4 ml (per T-225) or 112 ml (per CF10) of 300 m*M* $CaCl_2$. This solution was gently added to an equal volume of 2× HEPES-buffered saline (HBS: 290 m*M* NaCl, 50 m*M* HEPES buffer, 1.5 m*M* Na_2HPO_4, pH 7.0) and immediately mixed by gentle inversion three times to form a uniform solution. This solution was immediately mixed with fresh DMEM–F12 containing 10% FBS outside the flasks to produce a homogeneous plasmid solution mixture. Subsequently, medium in the

culture flasks was entirely replaced with this plasmid solution mixture. At the end of incubation for 6 hr, the plasmid solution mixture in the culture flasks was replaced with prewarmed fresh DMEM–F12 containing 2% FBS. Cell suspensions were collected 72 hr after transfection and centrifuged at 300 × *g* for 10 min. Each cell pellet was resuspended in 2 ml (per T-225) or 56 ml (per CF10) of Tris-buffered saline (TBS: 100 m*M* Tris-HCl [pH 8.0], 150 m*M* NaCl). Recombinant AAV was harvested by three cycles of freeze–thawing of each resuspended pellet. Crude viral lysate was then purified twice by passage through a CsCl two-tier centrifugation gradient, as described previously (Okada *et al.*, 2002b). The viral stock was titrated by dot-blot hybridization of DNase I-treated stocks with plasmid standards. To confirm transgene expression with the propagated vector *in vivo*, 5-week-old male Sprague-Dawley rats were injected via the anterior tibial muscle with AAV1-EGFP (1×10^{11} genome copies per rat). Fifteen weeks after injection, the rats were sacrificed and expression was confirmed by fluorescence microscopy.

Statistical analysis

Statistical significance was determined on the basis of an unpaired, two-tailed *p* value and Student *t* test, and a *p* value less than 0.05 was considered significant.

RESULTS

Improved gas exchange and maintenance of pH in medium after recombinant adenovirus infection

Propagation of vectors was based on infection or transfection of 293 cells on a large scale. A minipump was connected to the gas inlet of the CF10 and placed inside the incubator, so that the atmosphere in the incubator, containing 5% CO_2, was circulated through the CF10. The gas flow for circulation through the CF10 was maintained at 500 ml/min. An appropriate gas flow rate was important to give a uniform distribution of the gas in the individual trays of the CF10. A flow less than 200 ml/min gave uneven distribution of the gas, and significantly influenced cell growth. Gas flow that was too high also disturbed the uniformity of cell density. Appropriate cell density and uniform distribution of cells are critical to achieve successful gene transduction. Application of active gassing significantly increased cell growth in the CF10 (Table 1). CO_2 concentrations in the media stayed at their initial levels when using either a T-225 or CF10 with active gassing (Fig. 1A). In contrast, the CO_2 concentration inside the CF10 increased subsequent to adenovirus infection in the absence of active gassing. The pH of culture medium in the CF10 with active gassing was close to that in the T-225 and significantly higher than that in the CF10 without active gassing (Fig. 1B).

Monitoring of cell numbers and time point for harvest

The glucose level was monitored as an index for tracing cell growth and cytopathic effect in the CF10 to avoid the necessity for a specialized microscope to monitor cells in the large culture vessel. The glucose level decreased with increasing cell confluency and progression of cytopathic effect (CPE) (Fig. 2). When 80% CPE was reached, the glucose level was reduced to about 50 mg/ml. When glucose levels were less than 25%, the cells showed full CPE and this was regarded as the appropriate time for harvest.

Improved adenovirus vector production in a large culture vessel with active gassing

We estimated the adenovirus vector yield propagated by using 28 T-225 flasks with a surface area of 225 cm^2, a CF10 with a surface area of 6320 cm^2, or a CF10 in the presence of active gassing. When active gassing was used with the CF10, the productivity of the adenovirus vectors was dramatically increased, by 53.4 times compared with that in the CF10 without active gassing (Fig. 3). The vector yield per producer cell in the CF10 was also significantly improved in the presence of active gassing (Table 1). The PFU-to-particle ratios for vectors produced in the T-225, CF10, and CF10 with active gassing were 1:7, 1:15, and 1:10, respectively.

Efficient AAV vector production in a large culture vessel with active gassing

Enhanced gas exchange in a large culture vessel should also improve vector production through plasmid transfection. AAV vectors were produced in a large vessel by a three-plasmid transfection adenovirus-free protocol (Okada *et al.*, 2002b). Three days after plasmid transfection, the CO_2 concentrations in medium from the CF10 in the presence of active gassing were significantly less than those without active gassing (Table 2). The pH of the culture medium in the CF10 with active gassing was also improved. The CF-10 with active gassing was compatible with the three-plasmid transfection protocol for recombinant AAV production. When we used active gassing, the vec-

TABLE 1. INCREASED CELL GROWTH AND VECTOR YIELD WITH ACTIVE CO_2 AND AIR EXCHANGE[a]

Flask	*Number of cells harvested*	*Vector yield per cell (PFU/cell)*
225-cm^2 flask	$(1.4 \pm 0.2) \times 10^9$ (per 28 flasks)	7.9×10^3
CF10	$(4.9 \pm 1.6) \times 10^8$	4.1×10^2
CF10 + AG	$(1.3 \pm 0.3) \times 10^9$	8.2×10^3

[a]At the time of cell harvest after adenovirus infection, cell growth and vector yield per cell in a CF10 with a surface area of 6320 cm^2 in the presence or absence of active gassing (AG) were compared with that in 28 flasks with a surface area of 225 cm^2 each.

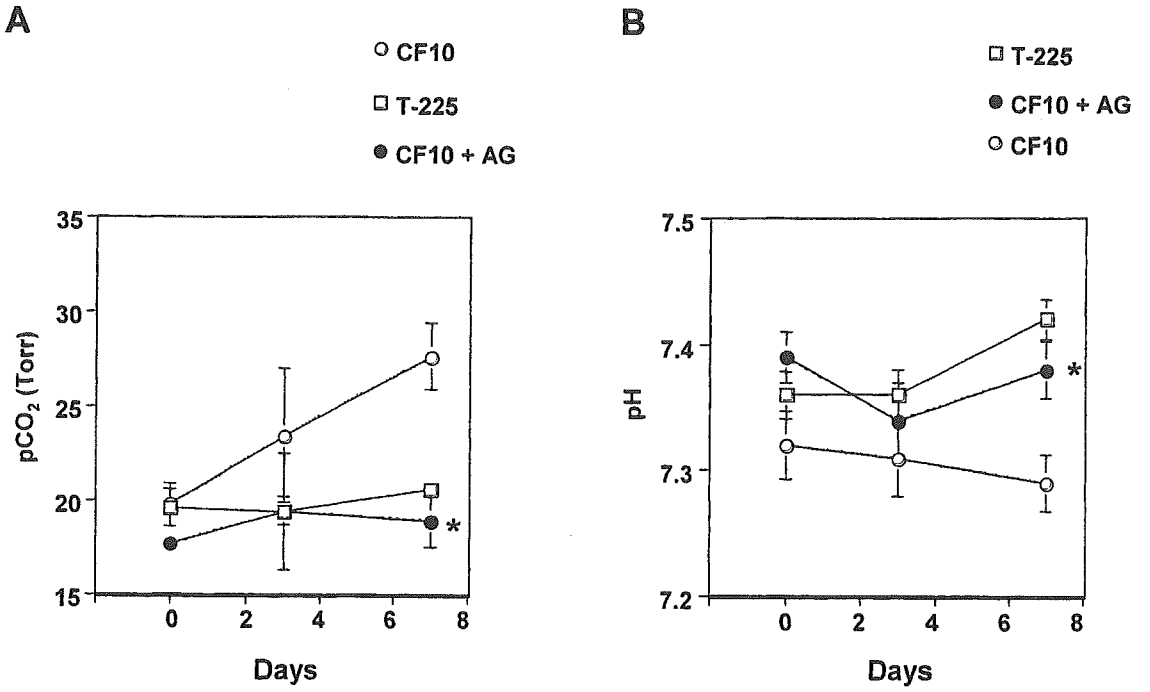

FIG. 1. Improved CO_2 and air exchange and maintenance of pH in conditioned medium after recombinant adenovirus infection. Subsequent to adenovirus infection in a normal flask with a surface area of 225 cm^2 (T-225) or a large culture vessel (a 10-tray Cell Factory [CF10] with a surface area of 6320 cm^2) in the presence or absence of active gassing (AG), CO_2 concentrations (**A**) and pH (**B**) in conditioned medium were determined ($n = 4$). Asterisk indicates $p < 0.05$ in comparison with a CF10 without AG.

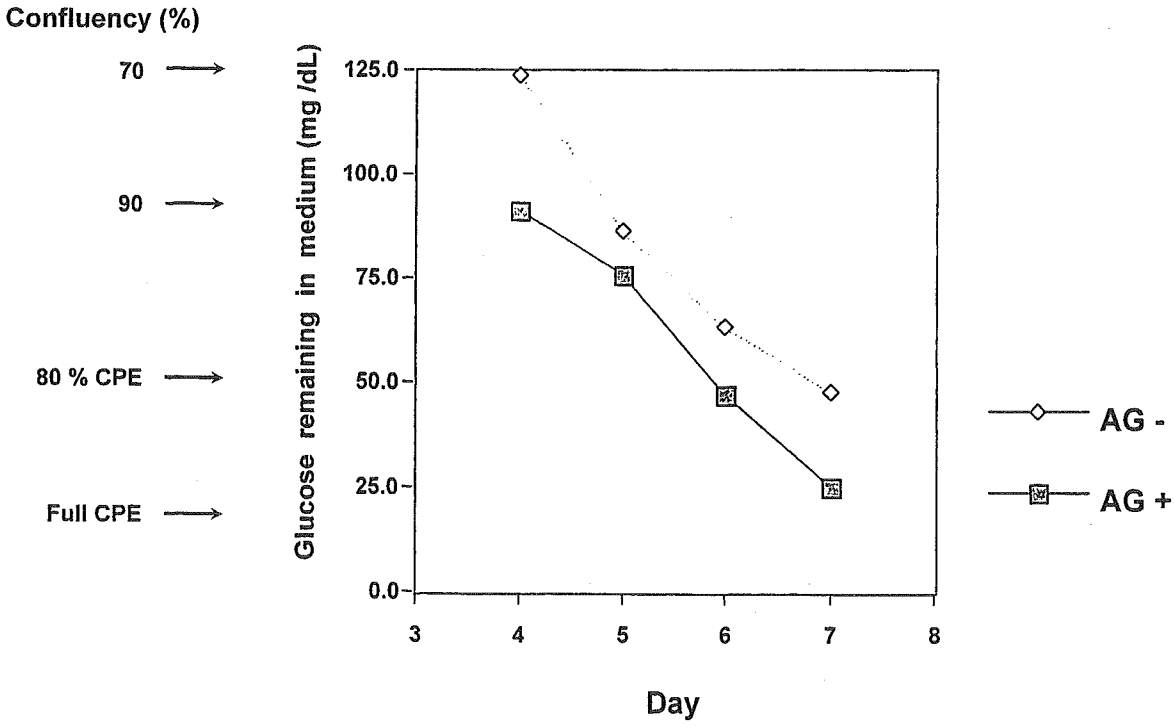

FIG. 2. Glucose reading to monitor cell growth. Glucose reading of culture medium was used as an index to monitor cell growth and cytopathic effect (CPE) in the CF10 to avoid the need for a specialized microscope. Cells were infected with recombinant adenovirus in the presence or absence of active gassing (AG) when 90% confluent.

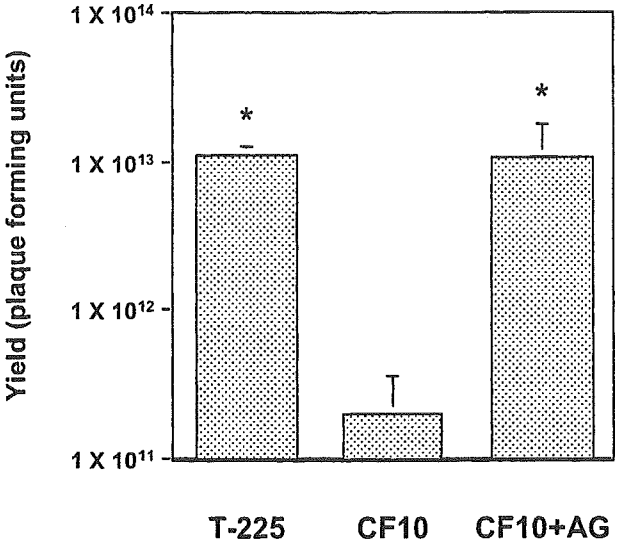

FIG. 3. Improved production of adenovirus vector. Adenovirus vector was propagated in 28 T-225 flasks ($n = 4$), a CF10 ($n = 3$), or a CF10 in the presence of active gassing (CF10 + AG, $n = 3$). Adenovirus vector expressing an EGFP reporter gene was generated in two independent experiments. The average number of plaque-forming units (PFU) was assessed by $TCID_{50}$. $^*p < 0.05$ in comparison with a CF10 without AG.

tor yield per cell was increased significantly, by 3.5 times (Table 3). Although vector yield was dependent on the transgene and construct, production of vector particles at up to 2.0×10^{13} genome copies per CF-10 was achieved.

Transduction of muscles with AAV vectors produced in a large culture vessel with active gassing

Five-week-old male Sprague-Dawley rats were injected with AAV1-enhanced green fluorescence protein (EGFP) (1×10^{11} genome copies per rat) via the anterior tibial muscle. Fifteen weeks after injection, the rats were sacrificed to confirm expression by fluorescence microscopy. The injected sites showed efficient expression of EGFP (Fig. 4).

TABLE 2. ENHANCED GAS EXCHANGE AND MAINTENANCE OF pH IN CONDITIONED MEDIUM AFTER PLASMID TRANSFECTION[a]

	pCO_2 (Torr)	*pH*
CF10	25.6 ± 1.1	7.23 ± 0.03
CF10 + AG	14.2 ± 0.1	7.40 ± 0.01

[a]Three days after plasmid transfection by using CF10 in the presence or absence of active gassing (AG), CO_2 concentrations and pH in the conditioned medium were estimated. Means ± standard deviations are shown ($n = 4$).

TABLE 3. IMPROVED YIELDS OF RECOMBINANT AAV TYPE 1 BY ACTIVE GAS EXCHANGE[a]

	Yield per vessel	*Yield per cell*
CF10	$(2.2 \pm 0.5) \times 10^{12}$	$(3.1 \pm 0.6) \times 10^{3}$
CF10 ± AG	$(1.0 \pm 0.7) \times 10^{13}$	$(1.1 \pm 0.7) \times 10^{4}$

[a]Titers of AAV1-EGFP were determined as genome copies by dot-blot analysis of DNase-treated stocks. AG, active gassing. Means ± standard deviations are shown ($n = 4$).

DISCUSSION

Successful vector production in a large culture vessel was achieved by improvement of CO_2 and air exchange along with maintenance of pH in the medium. Adenovirus production was enhanced by more than 50 times with the active gassing sys-

FIG. 4. Transduction of muscles with AAV vectors *in vivo*. Five-week-old male Sprague-Dawley rats were injected with AAV1-EGFP (1×10^{11} genome copies per body) via the anterior tibial muscle. Fifteen weeks after injection, the rats were killed to confirm expression by fluorescence microscopy. Scale bar: 100 μm.

tem. CF-10 with active gassing was also compatible with the three-plasmid transfection protocol for recombinant AAV production. When we used active gassing, the productivity of the AAV vectors was significantly increased.

In a direct comparison with vectors generated in ordinary culture flasks, viruses from the CF10 with active gassing were equivalent regarding function and bioactivity. The use of a CF10 with active gassing thus resulted in the production of vectors equivalent to those obtained in conventional culture dishes, but with a dramatically reduced workload. An average yield of approximately 1.0×10^{13} PFU requires as many as 28 T-225 flasks, according to our previous protocol. Alternatively, only one CF10 with active gassing was enough to achieve the same amount of virus. Furthermore, the PFU-to-particle ratio was also increased with the use of active gassing, suggesting improved bioactivity of the viruses. We used this system to amplify various adenovirus vectors. Although vector yield was dependent on the transgene and construct, a proportional increase in yield relative to surface area was achieved (data not shown).

The system was also compatible with plasmid transfection for recombinant AAV production. Active gassing combined with a large culture vessel significantly increased the productivity of the AAV vectors. The effect of enhanced gas exchange on the productivity of AAV vectors was less than the effect on the productivity of adenovirus vectors. Because lactate production accompanied by adenovirus replication is much greater than that with AAV, the protection of cells against pH drop by maintaining the CO_2 tension might be a plausible explanation for the preferential effect on adenovirus production. Transient transfection in a large culture vessel also provides a simple and flexible method of producing lentivirus-based vectors (Karolewski *et al.*, 2003). Therefore, our protocol would also be applicable to the efficient production of lentivirus- or retrovirus-based vectors.

Because this system fits into existing incubators and current vessels can readily be converted to the active gassing system, the viral production protocol using a CF-10 coupled with active gassing has practical utility for growing recombinant virus stocks in a limited laboratory space. This system has proven successful in our repeated manipulations and appears particularly promising. We have used the CF10 with the active gassing system in more than 400 vector preparations in the course of our more recent gene therapy experiments. The system allows us to perform a considerable number of *in vivo* experiments and to validate our studies.

ACKNOWLEDGMENTS

The authors thank Dr. Villy Nielsen, Ph.D. (Nunc, Roskilde, Denmark) and Mr. Hiroyuki Sano (Nalge Nunc International, Japan) for helpful discussions. We thank Avigen (Alameda, CA) for providing pAAV-LacZ and pAdeno. We thank Dr. Thomas Hope (University of Illinois at Chicago) for providing pBluescript II SK(+)WPRE-B11 and Dr. Jun-ichi Miyazaki (Osaka University Graduate School of Medicine, Japan) for pCAGGS. We also thank Ms. Miyoko Mitsu and Mr. Masataka Takahashi (Ieda Chemicals, Japan) for their encouragement and technical support. This study was supported in part by grants from the Ministry of Health, Labor, and Welfare of Japan; Grants-in-Aid for Scientific Research; a grant for the 21st Century Center of Excellence Program; and a matching fund subsidy from the High-Tech Research Center Project for Private Universities, through the Ministry of Education, Culture, Sports, Science, and Technology of Japan.

REFERENCES

BERGER, T.G., FEUERSTEIN, B., STRASSER, E., HIRSCH, U., SCHREINER, D., SCHULER, G., and SCHULER-THURNER, B. (2002). Large-scale generation of mature monocyte-derived dendritic cells for clinical application in cell factories. J. Immunol. Methods **268,** 131–140.

ITO, A., OKADA, T., MIZUGUCHI, H., HAYAKAWA, T., MIZUKAMI, H., KUME, A., TAKATOKU, M., KOMATSU, N., HANAZONO, Y., and OZAWA, K. (2003). A soluble CAR–SCF fusion protein improves adenoviral vector-mediated gene transfer to c-Kit-positive hematopoietic cells. J. Gene Med. **5,** 929–940.

KAROLEWSKI, B.A., WATSON, D.J., PARENTE, M.K., and WOLFE, J.H. (2003). Comparison of transfection conditions for a lentivirus vector produced in large volumes. Hum. Gene Ther. **14,** 1287–1296.

LIU, Y., OKADA, T., SHEYKHOLESLAMI, K., SHIMAZAKI, K., NOMOTO, T., MURAMATSU, S., KANAZAWA, T., TAKEUCHI, K., AJALLI, R., MIZUKAMI, H., KUME, A., ICHIMURA, K., and OZAWA, K. (2005). Specific and efficient transduction of cochlear inner hair cells with recombinant adeno-associated virus type 3 vector. Mol. Ther. (in press).

LIU, Y.L., WAGNER, K., ROBINSON, N., SABATINO, D., MARGARITIS, P., XIAO, W., and HERZOG, R.W. (2003). Optimized production of high-titer recombinant adeno-associated virus in roller bottles. Biotechniques **34,** 184–189.

MOCHIZUKI, S., MIZUKAMI, H., KUME, A., MURAMATSU, S., TAKEUCHI, K., MATSUSHITA, T., OKADA, T., KOBAYASHI, E., HOSHIKA, A., and OZAWA, K. (2004). Adeno-associated virus (AAV) vector-mediated liver- and muscle-directed transgene expression using various kinds of promoters and serotypes. Gene Ther. Mol. Biol. **8,** 9–18.

NOMOTO, T., OKADA, T., SHIMAZAKI, K., MIZUKAMI, H., MATSUSHITA, T., HANAZONO, Y., KUME, A., KATSURA, K., KATAYAMA, Y., and OZAWA, K. (2003). Distinct patterns of gene transfer to gerbil hippocampus with recombinant adeno-associated virus type 2 and 5. Neurosci. Lett. **340,** 153–157.

OKADA, T., RAMSEY, W.J., MUNIR, J., WILDNER, O., and BLAESE, R.M. (1998). Efficient directional cloning of recombinant adenovirus vectors using DNA–protein complex. Nucleic Acids Res. **26,** 1947–1950.

OKADA, T., NOMOTO, T., SHIMAZAKI, K., LIJUN, W., LU, Y., MATSUSHITA, T., MIZUKAMI, H., URABE, M., HANAZONO, Y., KUME, A., MURAMATSU, S., NAKANO, I., and OZAWA, K. (2002a). Adeno-associated virus vectors for gene transfer to the brain. Methods **28,** 237–247.

OKADA, T., SHIMAZAKI, K., NOMOTO, T., MATSUSHITA, T., MIZUKAMI, H., URABE, M., HANAZONO, Y., KUME, A., TOBITA, K., OZAWA, K., and KAWAI, N. (2002b). Adeno-associated viral vector-mediated gene therapy of ischemia-induced neuronal death. Methods Enzymol. **346,** 378–393.

OKADA, T., CAPLEN, N.J., RAMSEY, W.J., ONODERA, M., SHIMAZAKI, K., NOMOTO, T., AJALLI, R., WILDNER, O., MORRIS, J., KUME, A., HAMADA, H., BLAESE, R.M., and OZAWA, K. (2004). *In situ* generation of pseudotyped retroviral progeny by adenovirus-mediated transduction of tumor cells enhances the killing effect of HSV-tk suicide gene therapy *in vitro* and *in vivo*. J. Gene Med. **6,** 288–299.

TUYAERTS, S., NOPPE, S.M., CORTHALS, J., BRECKPOT, K., HEIRMAN, C., DE GREEF, C., VAN RIET, I., and THIELEMANS,

K. (2002). Generation of large numbers of dendritic cells in a closed system using Cell Factories. J. Immunol. Methods **264,** 135–151.

YAMAGUCHI, T., OKADA, T., TAKEUCHI, K., TONDA, T., OHTAKI, M., SHINODA, S., MASUZAWA, T., OZAWA, K., and INABA, T. (2003). Enhancement of thymidine kinase-mediated killing of malignant glioma by BimS, a BH3-only cell death activator. Gene Ther. **10,** 375–385.

YOSHIOKA, T., OKADA, T., MAEDA, Y., IKEDA, U., SHIMPO, M., NOMOTO, T., TAKEUCHI, K., NONAKA-SARUKAWA, M., ITO, T., TAKAHASHI, M., MATSUSHITA, T., MIZUKAMI, H., HANAZONO, Y., KUME, A., OOKAWARA, S., KAWANO, M., ISHIBASHI, S., SHIMADA, K., and OZAWA, K. (2004). Adeno-associated virus vector-mediated interleukin-10 gene transfer inhibits atherosclerosis in apolipoprotein E-deficient mice. Gene Ther. **11,** 1772–1779.

Address reprint requests to:
Dr. Takashi Okada
Division of Genetic Therapeutics
Center for Molecular Medicine
Jichi Medical School
3311-1 Yakushiji
Minami-Kawachi, Tochigi 329-0498, Japan

E-mail: tokada@jichi.ac.jp

Received for publication May 17, 2005; accepted after revision August 8, 2005.

Published online: September 21, 2005.

doi:10.1016/j.ymthe.2005.03.021

ARTICLE

Specific and Efficient Transduction of *Cochlear* Inner Hair Cells with Recombinant Adeno-associated Virus Type 3 Vector

Yuhe Liu,[1,2] Takashi Okada,[1] Kianoush Sheykholeslami,[3] Kuniko Shimazaki,[4] Tatsuya Nomoto,[1] Shin-Ichi Muramatsu,[5] Takeharu Kanazawa,[6] Koichi Takeuchi,[7] Rahim Ajalli,[2] Hiroaki Mizukami,[1] Akihiro Kume,[1] Keiichi Ichimura,[2] and Keiya Ozawa[1,*]

[1]*Division of Genetic Therapeutics, Center for Molecular Medicine, Jichi Medical School, 3311-1 Yakushiji, Minami-kawachi, Kawachi, Tochigi 329-0498, Japan*
[2]*Department of Otolaryngology and Head and Neck Surgery, Jichi Medical School, 3311-1 Yakushiji, Minami-kawachi, Kawachi, Tochigi 329-0498, Japan*
[3]*Department of Neurobiology, Northeastern Ohio Universities College of Medicine, Rootstown, OH 44272, USA*
[4]*Department of Physiology, Jichi Medical School, 3311-1 Yakushiji, Minami-kawachi, Kawachi, Tochigi 329-0498, Japan*
[5]*Department of Medicine, Division of Neurology, Jichi Medical School, 3311-1 Yakushiji, Minami-kawachi, Kawachi, Tochigi 329-0498, Japan*
[6]*Department of Otolaryngology and Head and Neck Surgery, Faculty of Medicine, University of the Ryukyus, Okinawa 903-0213, Japan*
[7]*Department of Anatomy, Jichi Medical School, 3311-1 Yakushiji, Minami-kawachi, Kawachi, Tochigi 329-0498, Japan*

**To whom correspondence and reprint requests should be addressed. Fax: (+81) 285 44 8675. E-mail: kozawa@jichi.ac.jp.*

Available online 12 May 2005

Recombinant adeno-associated virus (AAV) vectors are of interest for cochlear gene therapy because of their ability to mediate the efficient transfer and long-term stable expression of therapeutic genes in a wide variety of postmitotic tissues with minimal vector-related cytotoxicity. In the present study, seven AAV serotypes (AAV1–5, 7, 8) were used to construct vectors. The expression of EGFP by the chicken β-actin promoter associated with the cytomegalovirus immediate-early enhancer in cochlear cells showed that each of these serotypes successfully targets distinct cochlear cell types. In contrast to the other serotypes, the AAV3 vector specifically transduced cochlear inner hair cells with high efficiency *in vivo*, while the AAV1, 2, 5, 7, and 8 vectors also transduced these and other cell types, including spiral ganglion and spiral ligament cells. There was no loss of cochlear function with respect to evoked auditory brain-stem responses over the range of frequencies tested after the injection of AAV vectors. These findings are of value for further molecular studies of cochlear inner hair cells and for gene replacement strategies to correct recessive genetic hearing loss due to monogenic mutations in these cells.

Key Words: adeno-associated virus, serotype, gene transfer, cochlea, hair cells

INTRODUCTION

The total number of hair cells in the cochlea is finite. They are not renewed and there is very little (if any) redundancy in this population. The irreversible loss of cochlear hair cells is presumed to be a fundamental cause of permanent sensorineural hearing loss. Gene transfer into hair cells presents numerous opportunities for protecting these cells. There is considerable interest in the development of viral vectors to deliver genes to the cochlea to counteract hearing impairment, and recent studies have focused on vectors based on adenovirus [1–3], herpes simplex virus [4–6], lentivirus [7], and adeno-associated virus (AAV) [8,9]. The patterns of vector-encoded transgene expression have been found to differ significantly among vectors. Cochlear hair cells can be efficiently transduced with adenovirus vectors [10–12]. However, these vectors were found to provoke a strong immune response that could damage recipient cells and compromise cochlear function [10,13,14]; they are also incapable of mediating prolonged transgene expression [15,16]. Although AAV vectors might overcome these problems, the transduction of hair cells by AAV2-derived vectors is controversial [8,10,17]. To our knowledge, other AAV serotypes have not yet been tested as cochlear gene transfer vectors *in vitro* or *in vivo*. AAV vectors are of interest in the context of gene therapy because they mediate efficient transfer and long-term stable expression of therapeutic genes in a wide variety of postmitotic tissues with minimal vector-related cytotoxicity.

In this study, we assessed the utility of seven AAV serotypes as vectors with the chicken β-actin promoter associated with a cytomegalovirus immediate-early

Copyright © The American Society of Gene Therapy
1525-0016/$30.00

doi:10.1016/j.ymthe.2005.03.021

enhancer (CAG)-driven enhanced green fluorescent protein (EGFP) gene [18] in the murine cochlea. Vectors were introduced by microinjection through the round window membrane [19]. As a result, we determined that the specific and efficient gene transduction of inner hair cells could be achieved by using AAV type 3 vectors.

RESULTS

Expression Profile of EGFP in the Cochlea

Several cell types line the cochlear duct and support the hair cells (Fig. 1A). We carefully made a small opening in the tympanic bulla and injected vectors derived from the AAV1–4, 7, and 8 pseudotypes into the cochlea of two strains of mice (C57BL/6J and ICR) through the round window membrane (Fig. 1B). The mode of EGFP expression in various murine cochlear hair cells had a close similarity and was essentially equal for both strains. We determined the distribution of AAV vector-mediated EGFP expression throughout the cochlea for all serotypes tested (Table 1). A principal finding is that the inner hair cells in the organ of Corti showed clear evidence of EGFP expression with all of the AAV serotype-derived vectors except for the AAV4 vector (Fig. 2). This result indicates that most of the vectors (AAV1–5, 7, and 8) could efficiently transduce cochlear inner hair cells *in vivo* when slowly infused into the scala tympani. The AAV3-based vector was the most efficient and specific of the serotypes in transducing cochlear inner hair cells (Fig. 3). Transduction with 5×10^{10} genome copies (gc)/cochlea of the AAV3 vector resulted in robust transgene expression in the inner hair cells. The spiral ganglion cells showed significantly higher levels of fluorescence per unit area with the AAV5-based vector (Fig. 2n), and the spiral ligament cells were transduced prominently with the AAV1 and AAV7 vectors (Figs. 2d and 2r). Histological sections of cochleae injected with the AAV4 vector identified EGFP-positive cells predominantly in connective tissue within the mesothelial cells beneath the organ of Corti and in mesenchymal cells lining the perilymphatic fluid spaces (Figs. 2j and 2l). Furthermore, we detected intense expression with the AAV5- and AAV8-based vectors in the inner sulcus cells and in Claudius' cells (Figs. 2p and 2x). We did not detect notable levels of gene expression in the outer hair cells, supporting pillar cells, or stria vascularis cells for any serotype.

Long-term Expression of EGFP

We examined cochlear expression of the EGFP transgene in animals sacrificed at 1–12 weeks. Expression persisted in cochlear tissues for up to 3 months after infusion, while the extent of expression peaked at 2 weeks.

Transgene Activity

We determined the percentage of inner hair cells transduced with the AAV3 vector. The mid- to high-frequency regions of the cochlea were efficiently transduced, as shown in Fig. 3. Almost all of the inner hair cells in the basal and middle cochlear regions were transduced with the AAV3 vector (Fig. 4). Transgene expression was not detected in the hair cells of the apical turn of the cochlea. The predominant expression in the middle and basal cochlear turns is reasonable, as the virus

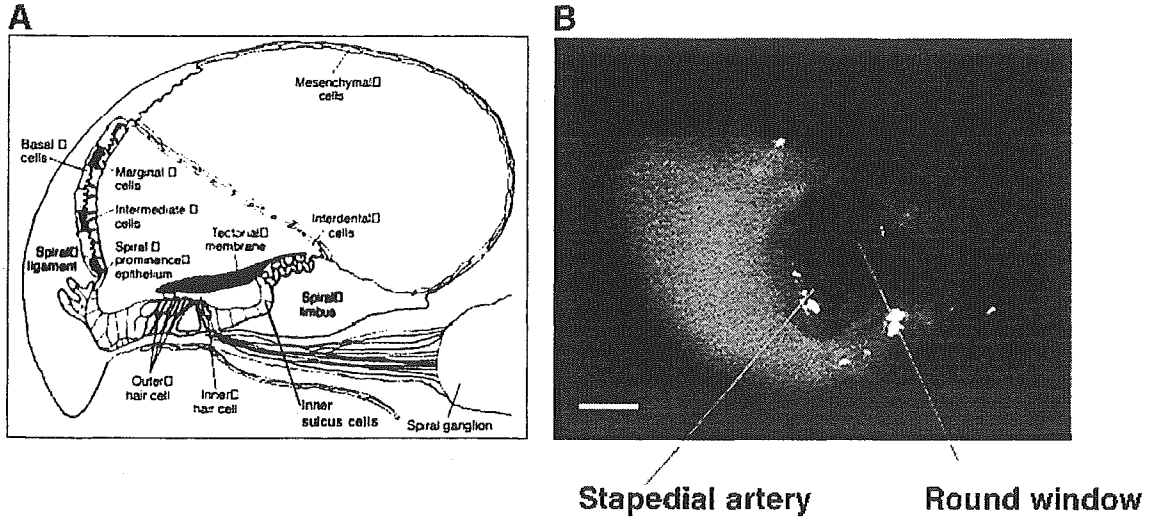

FIG. 1. (A) Schematic diagram of a cross section of the cochlea, demonstrating the scala vestibuli, scala tympani, and scala media or cochlear duct. The organ of Corti rests on the basilar membrane, with the hair cell cilia embedded in the gelatinous tectorial membrane. The outer margin of the cochlear duct contains the stria vascularis. Reproduced, by permission of the publisher, from [44]. (B) Direct visualization of the round window membrane in the right ear. The upper side of the picture is the back of the mouse and the right side is the head of the animal. The stapedial artery, a branch of the internal carotid artery, transverses an open bony semicanal within the round window niche. Bar denotes 500 μm, 15× original magnification.

Copyright © The American Society of Gene Therapy

TABLE 1: Expression of transgene in the mouse cochlea with vectors derived from the AAV1–4, 7, and 8 pseudotypes

Vector	Inner hair cells	Outer hair cells	Spiral ganglion	Stria vascularis	Spiral ligament	Spiral limbus	Reissner's membrane	Inner and outer pillar cells	Inner sulcus cells	Deiter's cells	Claudius' cells	Hensen's cells	Mesenchymal cells
AAV1	+++	–	++	–	++	++	++	–	+	–	–	–	++
AAV2	++	–	+	–	+	+	–	–	–	–	–	–	–
AAV3	++++	–	–	–	–	–	–	–	–	–	–	–	–
AAV4	–	–	–	–	–	–	–	–	–	–	–	–	+
AAV5	+++	–	+++	–	+	++	+	–	++	–	+	–	–
AAV7	+++	–	+	–	+++	++	–	–	+	–	+	–	++
AAV8	++++	–	–	–	+	+	–	–	++	–	+	–	+

The level of expression was graded by fluorescence intensity on a four-level scale (+, ++, +++, ++++) depending on the pixel/unit area count. ++++ means the strongest intensity of EGFP expression, + means the weakest intensity of EGFP expression, while – means no fluorescence.

was slowly infused into the scala tympani adjacent to the most basal turn of the cochlea. The percentage of transduced inner hair cells from the basal (high frequencies) to the apical (low frequencies) cochlear regions is shown in Fig. 4.

Cytotoxicity

We detected no deleterious effects on the viability of transduced cells. We compared evoked auditory brainstem response (ABR) threshold levels before and after injection, using a two-way repeated measure of the analysis of variance. There was no significant loss in ABR and hence no change in cochlear function for up to 10 days following vector infusion (Figs. 5A and 5B). In addition, the cellular and tissue architecture of experimental cochleae remained intact. There was no evidence of endolymphatic hydrops after AAV vector injection in any of the animals. We observed no significant destruction of the inner or outer hair cells (Fig. 5C).

Discussion

In the present study, we assessed the utility of vectors derived from seven AAV serotypes for gene delivery into the cochlea. Our results showed that the AAV3 vector was the most efficient and specific in transducing cochlear inner hair cells, although these cells could also be transduced with AAV1, 2, 5, 7, and 8 vectors. The transduction efficiency of the spiral ganglion by the AAV5 vector was particularly high, followed by that of the AAV1, AAV2, and AAV7 vectors. The efficient and specific transduction of inner hair cells with the AAV3 vector suggests that it recognizes a unique host range with a distinct cellular receptor. Transduction efficiency is dependent on initial viral binding (a property of the viral capsid), entry, and various postentry processes such as intracellular trafficking and second-strand synthesis [20–22]. The genome size of AAV vectors has also been demonstrated to affect transduction efficiency [23]. Comparisons of the serotypes have indicated that heterogeneity in the capsid-encoding regions and a differential ability to transduce cells may be associated with different receptor and co-receptor requirements for cell entry [24]. However, the receptors and co-receptors of AAV3 have not yet been clearly identified.

In the current study, we found that cochlear inner hair cells could be transduced with six AAV serotypes, although Lalwini *et al.* [8] reported that outer hair cells could be transduced with a low titer (1×10^6 viral particles/ml) of AAV2 *in vivo*. After injecting the AAV2 vector, we found that the spiral ganglion neurons, the inner hair cells, and the cells in the spiral ligament were all transduced. This transduction pattern differs from that reported in previous studies [8,10,17], and this discrepancy might be due to the different delivery methods and dissimilar promoters. Although the CAG promoter directs

Copyright © The American Society of Gene Therapy

doi:10.1016/j.ymthe.2005.03.021

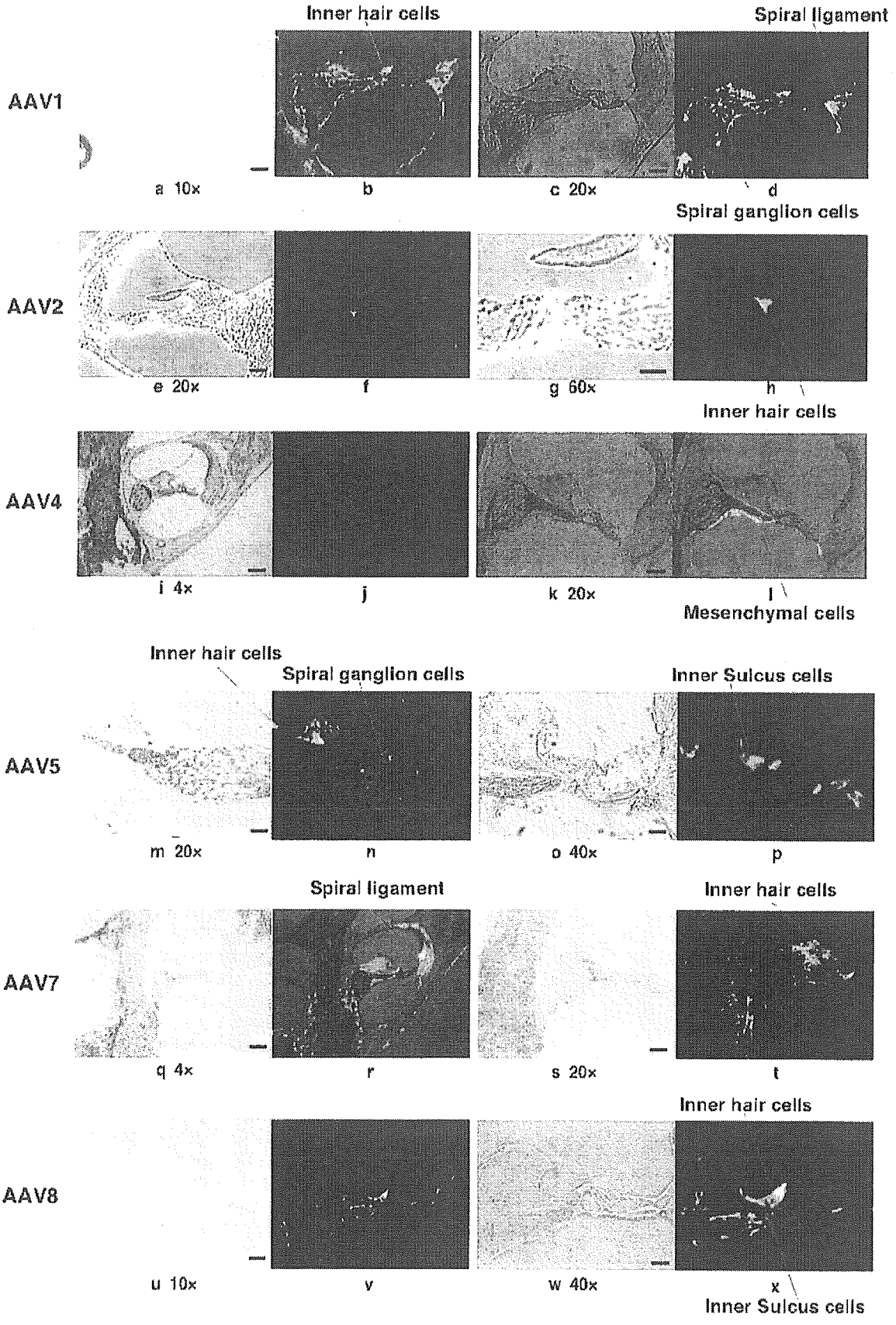

Copyright © The American Society of Gene Therapy

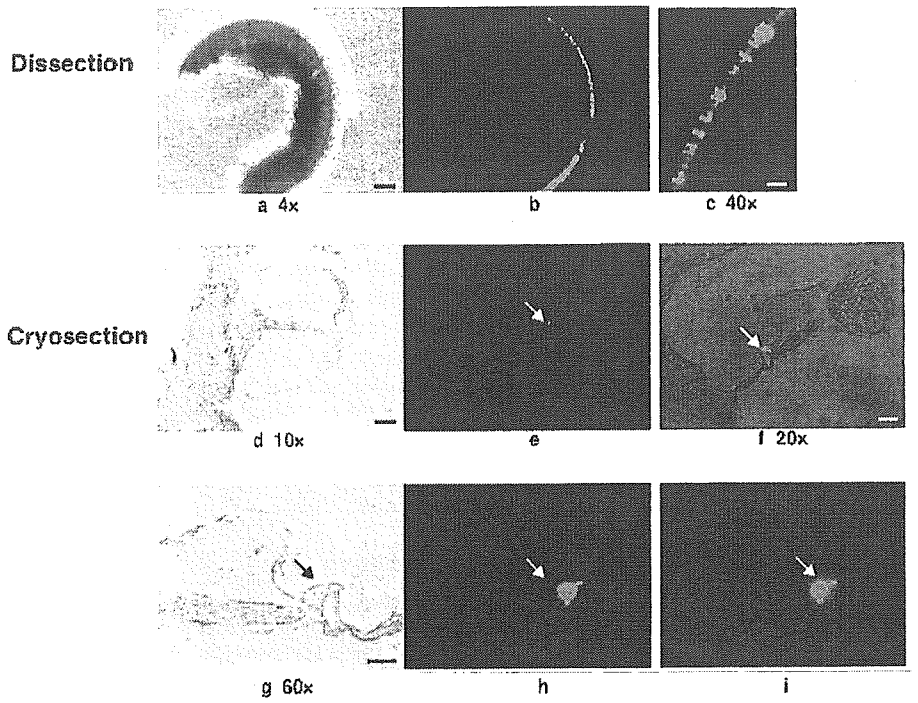

FIG. 3. Cochlear transduction with AAV3-CAG-EGFP. Dissected cochleae and cryosections show transgene expression in inner hair cells. (a) A light photomicrograph of the basal turn of the cochlea is shown, illustrating its laminar structure. (b) A fluorescence photomicrograph of this dissection. (c) A higher magnification view of the dissection shown in (b), illustrating a row of inner hair cells in the organ of Corti expressing EGFP. (d–i) Representative photomicrographs from three magnifications of a radial cochlear cryosection. (d) Light photomicrography of an intact cochlear duct. Fluorescence photomicrography of this duct is shown in (e). (h and i) A higher magnification of (e), illustrating EGFP expression within inner hair cells. Cryosections show transgene expression in the inner hair cells (arrows). Scale bars: 4×, 250 μm; 10×, 100 μm; 20×, 50 μm; 40×, 25 μm; 60×, 25 μm.

higher expression than do the cytomegalovirus (CMV) and EF-1α promoters [25], each promoter drives reporter gene expression in different cell types [26,27].

Cell-specific or -selective infectivity of the viral vectors suggests the presence of various factors to introduce the distinct expression patterns of the transgenes. Spiral ganglion neurons and glial cells can be transduced with a lentivirus–GFP construct *in vitro* but not *in vivo* [7]. The differential transducibility under *in vivo* and *in vitro* conditions reflects a high degree of structural isolation of the spiral ganglion and other cell types—such as the cells on the periphery of the endolymph—from the perilymph into which the viral vector was introduced. The strict separation of the endolymph from the perilymph is maintained by tight junctions that line the boundary between these fluid chambers. The size of the viral particle may contribute to the observed variability in transgene expression promoted by different vectors. The diameters of adenovirus and retrovirus (including lentivirus) particles are approximately 75 nm and greater than 100 nm, respectively, while the diameters of AAV vectors are typically 11–22 nm [28,29]. Thus, the larger size of lentiviruses and adenoviruses may limit their subsequent dissemination from the perilymph into the endolymph. The variable patterns of adenovirus- and lentivirus-mediated gene expression seen with different methods of inoculation may be due to the inoculation route, the volume and number of viral particles, differences in viral preparation, or differences in the method of transgene detection. The introduction of adenovirus vectors by cochleostomy or with an osmotic pump via the round window leads to a more efficient transduction of cochlear hair cells [30–32]. The apical domain (apical membrane and stereocilia) of cells in the sensory epithelium (hair cells and supporting cells) is bathed in endolymph, while the basal–lateral domain is immersed in perilymph. Access of the viral vectors to the endolymphatic space by cochleostomy may facilitate the transduction of hair cells and supporting cells. However, although the cochleostomy procedure has been tested, inoculation into the membranous labyrinth could not be confirmed [32]. In the present study, AAV vectors were found to infect cochlear hair cells easily *in vivo,* via round window injection.

Gene transfer into the cochlea through the round window membrane is ideal, because this procedure

FIG. 2. Transduction of the cochleae by AAV1-, AAV2-, AAV4-, AAV5-, AAV7-, and AAV8-based vectors. (a, c, e, g, i, k, m, o, q, s, u, and w) Light photomicrographs of cochlear cryosections. (b, d, f, h, j, l, n, p, r, t, v, and x) Fluorescence photomicrographs (green fluorescence from transgene). The spiral ligament cells were transduced prominently with the AAV1 and AAV7 vectors (d and r). Transgene expression in inner hair cells was detected with AAV1-, AAV2-, AAV5-, AAV7-, and AAV8-based vectors (b, h, n, t, and x). AAV4-based vector faintly transduced mesenchymal cells (j and l). The spiral ganglion cells showed significant levels of fluorescence with the AAV5-based vector (n). Intense fluorescence was detected with the AAV5- and AAV8-based vectors in the inner sulcus cells (p and x). Scale bars: 10×, 100 μm; 20×, 50 μm; 40×, 25 μm; 60×, 25 μm.

Copyright © The American Society of Gene Therapy

doi:10.1016/j.ymthe.2005.03.021

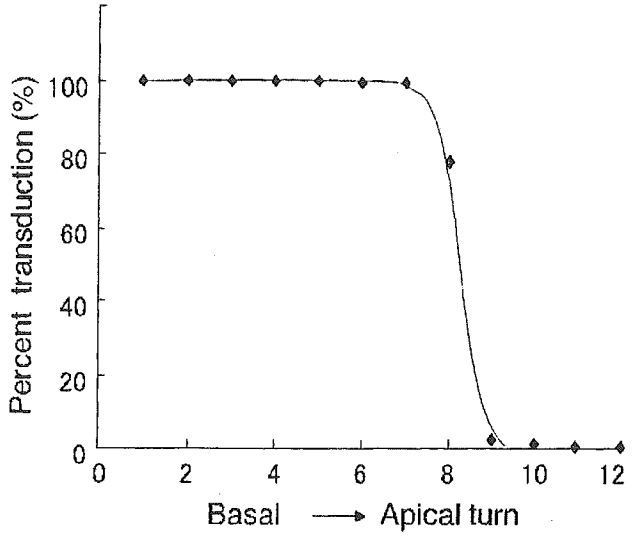

FIG. 4. EGFP expression profile of inner hair cells transduced with AAV3, as shown for a cross section subdivided into 12 segments ranging from the basal (high frequencies) to the apical (low frequencies) cochlear regions.

requires simple surgery without cochlear trauma [19]. Another critical factor in assessing the utility of a gene transfer vector is safety. Factors determining safety include the toxicity of the gene transfer agent itself, the provocation of immune responses, the generation of replication-competent virus, and the risk of creating genetically modified cells by insertional mutagenesis. The cells and tissues within the AAV-EGFP-perfused cochleae were free from inflammation and were generally intact. No pathological changes were observed in the organ of Corti, stria vascularis, or spiral ganglion cells. The long-term expression of EGFP within the cochlear tissues is consistent with data obtained from other animal models and different organ systems [9,33]. Since EGFP is known to introduce cellular toxicity, vectors expressing physiologically therapeutic proteins would achieve longer transduction periods than EGFP. Gene transfer into the inner hair cells presents numerous opportunities for auditory neuroscience. Potential applications include the localization of proteins by expression of tagged constructs, the generation of dominant-negative or antisense knockouts of endogenous proteins, the rescue of mutant phenotypes to identify disease genes, and perhaps even the treatment of auditory disorders. Advances in the molecular basis of auditory diseases have allowed the identification of a number of genetic disorders such as presbycusis, acoustic trauma, and ototoxicity. The development of gene therapy now allows us to evaluate the effects of transferring therapeutic genes into the inner ear by several different strategies. The expression of marker genes in the inner ear tissue has been demonstrated. Further studies will improve our understanding of cochlear function as well as provide for the development of novel therapies for a wide variety of inner ear diseases. Intracochlear gene transfer using AAV vectors has been established as a viable experimental proposition. Future study will include the transfer of functioning genes *in vivo* and the development of alternative vectors. While clinical application may be some way off, it is vital that gene delivery techniques are optimized in anticipation of future need.

In conclusion, the data presented in this paper demonstrate successful gene transfer into several types of cochlear cells *in vivo* with AAV-based vectors. Interestingly, the AAV3 vector promoted inner hair cell-specific transduction. These findings are of value for further molecular studies of the cochlear inner hair cells and for gene replacement strategies to correct hereditary hearing loss due to specific monogenic mutations affecting cochlear inner hair cells.

MATERIALS AND METHODS

Construction and preparation of proviral plasmids. The AAV vector proviral plasmid pAAV2-*LacZ* harbors an *Escherichia coli* β-galactosidase expression cassette with the CMV promoter, the first intron of the human growth hormone gene, and the SV40 early polyadenylation sequence, which are flanked by inverted terminal repeats (ITRs) [34]. The *LacZ* expression cassette of pAAV2-*LacZ* was ligated to *Not*I-excised pAAV5-RNL [35] to form the proviral plasmid pAAV5-*LacZ*. The pAAV2-CAG-EGFP-WPRE construct consists of the EGFP gene under the control of the CAG promoter (the chicken β-actin promoter associated with the cytomegalovirus immediate-early enhancer) and WPRE (woodchuck hepatitis virus posttranscriptional regulatory element) flanked by ITRs. The WPRE cassette augments the stability of transgene mRNA [36] and increases EGFP expression levels, thereby ensuring long-term transgene expression. A *Bam*HI–*Xba*I fragment containing the EGFP cDNA excised from pEGFP-1 and a *Hin*dIII fragment containing the WPRE sequence excised from pBS II SK$^+$WPRE-B11 (a gift from Dr. J. Donello) was ligated to *Xho*I linkers and cloned into an *Xho*I site of pCAGGS (a gift from Dr. J.-I. Miyazaki) to create pCAG-EGFP-WPRE. The EGFP expression cassette from pCAG-EGFP-WPRE was ligated to the *Not*I-excised pAAV2-*LacZ* and pAAV5-RNL [35] to form the proviral plasmids pAAV2-CAG-EGFP-WPRE and pAAV5-CAG-EGFP-WPRE, respectively. The AAV-helper plasmid harbors Rep and Cap. The adenovirus helper plasmid pAdeno5 (identical to pVAE2AE4-5) encodes the entire E2A and E4 regions and the VA RNA I and II genes [37]. Plasmids were purified with the Qiagen plasmid purification kits (Qiagen K.K., Tokyo, Japan).

Recombinant AAV vector production. Vectors derived from the AAV1–4, 7, and 8 pseudotypes were produced with the AAV packaging plasmid pAAV1RepCap (for AAV1) [38], pHLP19 (for AAV2), pAAV3RepCap (for AAV3) [39], pAAV4RepCap (for AAV4) [40], pAAV7RepCap (for AAV7) [41], or pAAV8RepCap (for AAV8) [41] and the AAV proviral plasmid pAAV2-*LacZ* or pAAV2-CAG-EGFP-WPRE. The plasmids pAAV5RepCap [35] and pAAV5-*LacZ*, or pAAV5-CAG-EGFP-WPRE, were used to produce vector with the AAV5 pseudotype [42]. Seven AAV serotype vectors were produced as previously described by the three-plasmid transfection adenovirus-free protocol [37]. Briefly, three days before transfection, 293 cells were plated onto a 10-tray Cell Factory (Nalge Nunc International, Rochester, NY, USA; 6×10^7 cells/10-tray). The cells were cotransfected with 650 μg each of the proviral plasmid, the AAV vector packaging plasmid, and the adenovirus helper plasmid pAdeno5 [34] by the calcium phosphate coprecipitation method. The medium was changed following incubation for 6–8 h at 37°C. Recombinant AAV was harvested 72 h after transfection by three freeze/thaw cycles. The crude viral lysate was purified twice on a cesium chloride two-tier centrifugation

Copyright © The American Society of Gene Therapy